Journal of Biomedical Optics

BiomedicalOptics.SPIEDigitalLibrary.org

Optimization of sapphire capillary needles for interstitial and percutaneous laser medicine

Irina N. Dolganova
Irina A. Shikunova
Gleb M. Katyba
Arsen K. Zotov
Elena E. Mukhina
Marina A. Shchedrina
Valery V. Tuchin
Kirill I. Zaytsev
Vladimir N. Kurlov

SPIE.

Irina N. Dolganova, Irina A. Shikunova, Gleb M. Katyba, Arsen K. Zotov, Elena E. Mukhina, Marina A. Shchedrina, Valery V. Tuchin, Kirill I. Zaytsev, Vladimir N. Kurlov, "Optimization of sapphire capillary needles for interstitial and percutaneous laser medicine," *J. Biomed. Opt.* **24**(12), 128001 (2019), doi: 10.1117/1.JBO.24.12.128001.

Optimization of sapphire capillary needles for interstitial and percutaneous laser medicine

Irina N. Dolganova,[a,b,c,*] Irina A. Shikunova,[a] Gleb M. Katyba,[a,c] Arsen K. Zotov,[a] Elena E. Mukhina,[c] Marina A. Shchedrina,[b] Valery V. Tuchin,[d,e,f,g] Kirill I. Zaytsev,[b,c,h] and Vladimir N. Kurlov[a,b,*]
[a]Russian Academy of Sciences, Institute of Solid State Physics, Chernogolovka, Russia
[b]Sechenov First Moscow State Medical University, Institute for Regenerative Medicine, Moscow, Russia
[c]Bauman Moscow State Technical University, Moscow, Russia
[d]Saratov State University, Saratov, Russia
[e]Russian Academy of Sciences, Institute of Precision Mechanics and Control, Saratov, Russia
[f]Tomsk State University, Tomsk, Russia
[g]ITMO University, St. Petersburg, Russia
[h]Russian Academy of Sciences, Prokhorov General Physics Institute, Moscow, Russia

Abstract. Sapphire capillary needles fabricated by edge-defined film-fed growth (EFG) technique hold strong potential in laser thermotherapy and photodynamic therapy, thanks to the advanced physical properties of sapphire. These needles feature an as-grown optical quality, their length is tens of centimeters, and they contain internal capillary channels, with open or closed ends. They can serve as optically transparent bearing elements with optical fibers introduced into their capillary channels in order to deliver laser radiation to biological tissues for therapeutic and, in some cases, diagnostic purposes. A potential advantage of the EFG-grown sapphire needles is associated with an ability to form the tip of a needle with complex geometry, either as-grown or mechanically treated, aimed at controlling the output radiation pattern. In order to examine a potential of the radiation pattern shaping, we present a set of fabricated sapphire needles with different tips. We studied the radiation patterns formed at the output of these needles using a He–Ne laser as a light source, and used intralipid-based tissue phantoms to proof the concept experimentally and the Monte-Carlo modeling to proof it numerically. The observed results demonstrate a good agreement between the numerical and experimental data and reveal an ability to control within wide limits the direction of tissue exposure to light and the amount of exposed tissue by managing the sapphire needle tip geometry. [DOI: 10.1117/1.JBO.24.12.128001]

Keywords: sapphire shaped crystals; laser thermal therapy; photodynamic therapy; medical instruments; medical needles; edge-defined film-fed growth.

Paper 190308R received Sep. 10, 2019; accepted for publication Nov. 26, 2019; published online Dec. 17, 2019.

1 Introduction

Laser radiation is widely applied in medical treatments,[1–3] particularly in photodynamic therapy (PDT) and laser thermal therapy (LTT), for achieving photochemical and photothermal effects in tissues aimed at destruction of malignant and benign neoplasms.[4,5] The general mechanism of PDT is a laser-radiation-induced activation of photosensitizers—i.e., special drugs introduced into patient's body and accumulated in pathological tissues. This leads to a photochemical reaction in the tissues, resulting in a generation of the cytotoxic products, such as singlet oxygen and other radicals.[6,7] In turn, LTT relies on a hyperthermia of tissues with their further ablation due to the light absorption in a tissue volume.[8] These methods are minimally invasive (i.e., they limit the size of tissue damage and thus reduce the healing time of wounds, associated pain, and the risk of infection), which makes them rather attractive in the modern treatment strategies. PDT is extensively applied for cancer treatment,[9–13] whereas LTT provides treatment of varicose vein,[14] lipolysis,[15] epilepsy,[16] as well as cancers of the skin,[8] pancreas,[17] liver,[18] prostate,[19] lung,[20] breast,[21] and brain.[22–24]

Both PDT and LTT admit interstitial application, turning into interstitial photodynamic therapy (I-PDT)[25–27] and laser interstitial thermal therapy (LITT),[28–30] aimed to deliver laser radiation directly to the internal region of interest (ROI) without an extensional surgical incision, using optical fibers.[2,6,31] A common technique for light delivery implies introduction of an optical fiber (or a bundle of fibers) into tissues via application of entirely or partly transparent needles or catheters, which are then usually removed in order to ensure a direct contact between a fiber and a tissue for increased photochemical and photothermal effects.[2] In some cases, fiber can be protected from interaction with aggressive biological environments, as well as from overheating by special caps or domes.[15,32] Such protectors often enable circulation of a liquid coolant,[20,33,34] but complicate the instrument as well. An essential aspect of LITT is that a volume of the tissue ablation is limited mainly by the maximal power of light source that can be applied without a carbonization of surrounded tissues.[35] The initial carbonization prevents from further penetration of light into deeper tissue regions, thus, reducing the ablation volume. Moreover, such overheated tissue regions initiate an undesirable fiber damage and the significant uncontrolled changes of the predicted distributions of light and heat.

Majority of modern instruments for LITT and I-PDT relies on silica optical elements (e.g., fibers, windows, and transparent

*Address all correspondence to Irina N. Dolganova, E-mail: in.dolganova@gmail.com; Vladimir N. Kurlov, E-mail: kurlov@issp.ac.ru

protective introducers),[6,27,36] which possess quite a limited radiation strength, rather low chemical resistance to the chemical composition of *in vivo* tissues, and low thermal resistance.[31] This limits the radiation power and the exposure duration, thus, reducing a potential of the silica-based instruments, particularly in LITT, where significant radiation power is required.[37,38] In order to mitigate this difficulty, sapphire has been recently considered as a favorable material platform for fabrication of the optical components of the interstitial irradiators.[37,39,40] Indeed, it possesses a unique combination of physical properties, which makes it attractive for the considered applications.[41]

- It is transparent in a broad range of electromagnetic spectrum, spanning the ultraviolet (partially), visible, infrared (partially), and terahertz ranges;
- It is nonmagnetic and demonstrates high hardness, heat resistance, and mechanical strength;
- It features an impressive chemical inertness and is capable of operation in aggressive media.

Most recently, an ability to fabricate sapphire capillary needles for the interstitial therapy using the edge-define film-fed growth (EFG) technique[42–44] has been proposed by our research group.[45] The sapphire needles grown by this technique directly from the Al_2O_3-melt demonstrate an as-grown high surface and bulk quality, the length of tens of centimeters, and have internal capillary channels. The EFG technique eliminates the use of crystal drilling, grinding, and polishing during fabrication of the sapphire needle and makes them much more technologically reliable, thanks to a reduction of both the fabrication duration and the instrument cost.

Despite the technological attractiveness of the EFG-grown sapphire capillary needles, there is still a need for optimization of their geometry for applications in the laser therapy, assuming interstitial and percutaneous exposure. In order to examine a potential of various geometries of the sapphire needle tip for shaping the output radiation pattern, in this paper, we present a set of fabricated needles featuring either as-grown or mechanically treated tips of different shapes, including conical, hypo- and hyper-hemispherical, parabolic, and drop-like ones. Then we perform experimental studies, involving the use of a He–Ne laser and a tissue phantom, and numerical analyses, based on statistical Monte-Carlo methods, in order to estimate and objectively compare the radiation patterns, formed at the needle tips. The observed results reveal an ability to control, within wide limits, the direction of tissue exposure and the amount of exposed tissues by managing the needle tip geometry. This justifies a bright future of sapphire capillary needles in the laser therapy technologies.

2 Fabrication of Sapphire Needles with Different Tips

An in-depth review of the EFG and related techniques can be found in Refs. 41 and 46–48. Here we briefly describe the crystal growth setup, which is schematically shown in Fig. 1(a). It uses a 22-kHz induction-heated graphite susceptor, a molybdenum crucible, and the Verneuil crystal as a feed material. The sapphire rod with capillary channel is grown from the melt Al_2O_3-film, formed on the top of a capillary die at the temperature of 2053°C and in an ambient high-purity Ar-atmosphere. The Ar pressure can be tuned in the range from 1.1 to 1.3 atm,

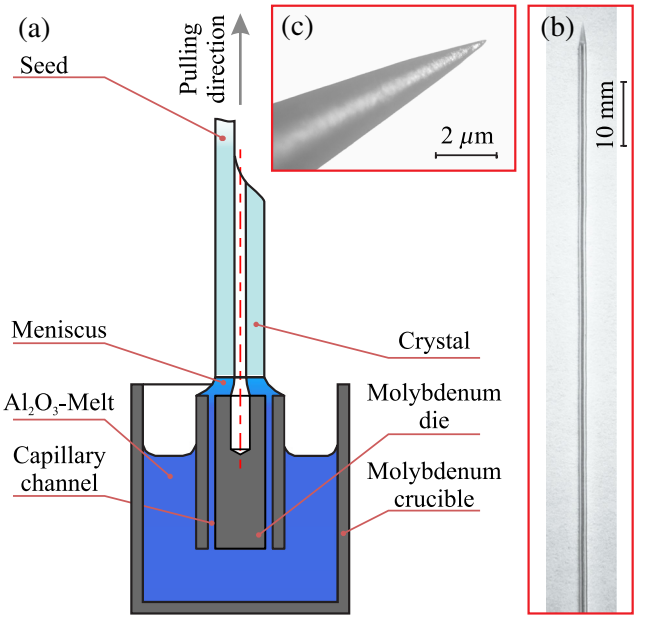

Fig. 1 Sapphire needle fabrication using the EFG technique: (a) a scheme of the growth process and pictures of the (b) sapphire needle and (c) its tip.

while the pulling rate is about 50 to 150 mm/h. During the growth process, an Al_2O_3-melt rises to the top of the die through a 0.1-mm-thick capillary channels. The crystal shape is mainly determined by the design of a die, while its small variations, originating from the surface tension of the melt in the meniscus region, are possible. Along with an ability to automatically maintain a stationary cross-section geometry with a high quality over the length of tens of centimeters (i.e., up to the atomically flat as-grown crystal surfaces), our modifications of the EFG technique yield formation of a complex as-grown crystal ends. Particularly, such geometries as hemisphere, hypo- and hyper-hemisphere, close-to-parabolic, or drop-like shapes of the needle tip are available.[48] Notice that the transition from the tubular crystal to the monolithic part is obtained in a single growth cycle. The as-grown tips are formed by an appropriate selection of the crystal growth parameters at the final stage of its pulling from the melt.

Using the described setup, we fabricate a set of sapphire needles, as shown in Fig. 2. The needles with the diameter of 1.2 mm are consisted of a sapphire body with a 500-μm-diameter capillary channel, intended for placing a optical fiber inside. The closed end of the capillary channel has a semispherical form with the radius depending on the technological parameters of the growing process, such as temperature, pressure, and pulling rate. The length of the needle can be larger than 200 mm. It is possible to make various tips of sapphire needles with or without mechanical shaping. The most common type for interstitial treatment is a pointed needle, which is shown in Figs. 1(b) and 2(a). Its cone angle can be changed by sharpening. In addition, it is possible to make other mechanically treated or as-grown ends of a needles, demonstrated in Fig. 2(b); they could be applied superficially, percutaneously, or interstitially. We should note that comparing to silica catheters, the surface quality, thermal and mechanical stability of such complex tips are higher.

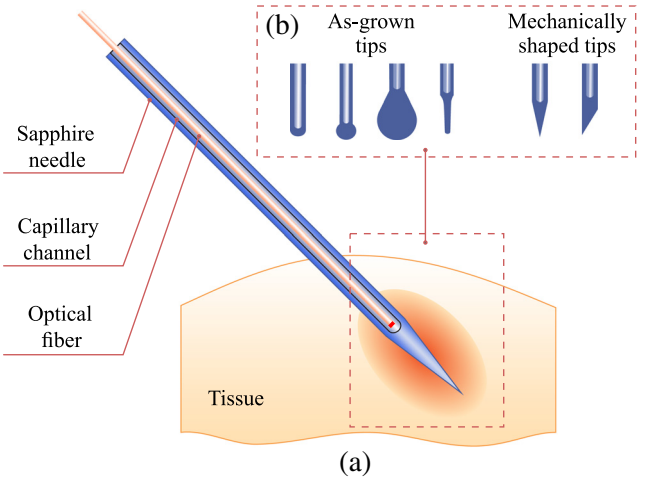

Fig. 2 A scheme of tissue exposure to laser radiation using a sapphire capillary needles with a complex tip: (a) a sapphire capillary needle introduced into tissue and (b) different geometries of the needle tip studied in this work.

3 Study of Radiation Patterns Formed by Sapphire Needles

In order to observe the radiation patterns, formed by the fabricated sapphire needles in tissues, we use a scheme presented in Fig. 3. A needle with a silica fiber (the numerical aperture is NA = 0.5, and the core diameter is 400 μm) connected to a He–Ne laser ($\lambda = 632.8$ nm) providing the power density of 400 mW/cm^2 on its flat end is introduced into a cuvette with 20% intralipid (Fresenius Kabi) solution diluted in a saline as 1:20 so that the tip is half below the intralipid surface. We do not apply special agents inside the capillary channel, therefore, the space between the fiber and sapphire is filled with the air and forms a special gap, which definitely impact on the light propagation. Indeed, introduction of some liquid agent between the silica fiber and the sapphire needle might sufficiently reduce the light scattering and Fresnel losses of laser energy inside the instruments. Nevertheless, these effects are difficult to classify at this time, and more investigations are in order.

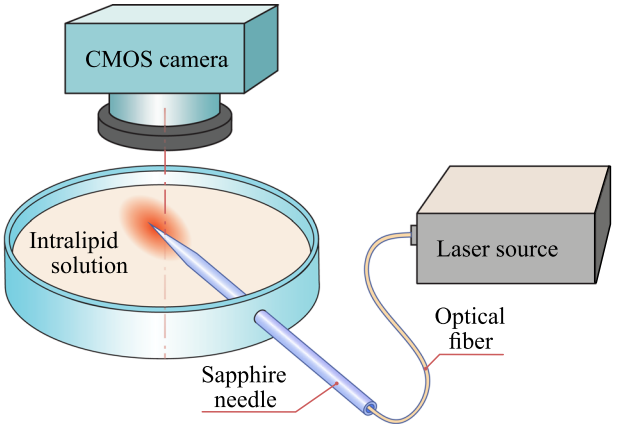

Fig. 3 A scheme of the experimental setup applied to study of the radiation patterns, which are formed at the needle tip. Here an intralipid solution forms a semitransparent scattering medium, which serves as a tissue phantom, while the needle body is handled slightly below the intralipid surface.

Images of a needle in an intralipid solution, which are taken in a dark room using a CMOS camera atop of the cuvette, are presented in Fig. 4(b), as compared to photos of the free-standing sapphire needles, shown in Fig. 4(a). From these images, we can observe the absolutely different distributions of laser radiation in a tissue phantom, from direct (types II, III, and IV) to aside (type VI) and diffuse (types I and V). It means that it is possible to obtain different heating and ablation tissue regions using such sapphire tips and a flat-faced fiber.

Additionally, we use a TracePro® package for the 3-D numerical simulation of photons' migration in the fiber, sapphire needle and intralipid solution, geometry and optical properties of which are chosen to be close to that observed in experiment, based on the radiative transfer equation and the Monte-Carlo simulations. The phantom has the refractive index of $n_p = 1.33$, the absorption coefficient of $\mu_a = 10^{-4}$ mm^{-1}, the scattering coefficient of $\mu_s = 0.2$ mm^{-1}, and Henyey–Greenstein scattering phase function with the anisotropy coefficient of $g = 0.5$.[49] These optical parameters are typical for intralipid solution at the He–Ne laser wavelength of $\lambda = 632.8$ nm.[49,50] The refractive indices of sapphire and silica fiber are 1.78 and 1.54, respectively, both have the small absorption coefficients of 10^{-6} mm^{-1} and 3×10^{-6} mm^{-1}, correspondingly.

In Figs. 4(c) and 4(d), the distributions of transmitted and absorbed light intensity in logarithmic-scale are shown for the considered sapphire tips. One could notice a good agreement between the numerical and experimental data. Evidently, these needles can have rather different applications. The type I features mostly diffused light with low anisotropy used for uniformly heating a large ROI. In contrast, the types II and III with hypo- and hyper-hemispherical tips, respectively, provide forward-propagated light with high anisotropy and feature diverging light beam. They possibly might be used for the treatment of small regions. Moreover, small amounts of radiation propagated in side directions, making these types suitable for superficial and percutaneous exposure. Nevertheless, the type II with small diameter might be applied interstitially for soft tissues. The type IV having a drop-like tip demonstrates rather uniform radiation pattern within a wide beam. We should stress that such a geometry provides some internal scattering, clearly observed in Fig. 4(a). It might originate from the residual defects and tensions in the crystal tip. Therefore, for this type, we observe differences between the numerical and experimental data. The drop-like tip can be applied for percutaneous treatment and admit exposure of rather large tissue area. The type V features a complex radiation pattern thanks to the parabolic form. It diffuses light, but in contrast to type I, has a strong forward-propagated component. Having a semipointed geometry, this type can be applied both percutaneously and interstitially. Meanwhile, types I and V could be rather promising in optogenetics for precise light delivery to the certain brain regions in order to stimulate neuronal activity.[51,52] Finally, due to the broken axial symmetry, an angle-cut sapphire tip of the type VI, unlike the other types, can be used for lateral irradiation, when direct access to the ROI is limited. For example, side irradiation is important for preventing damage of the neurovascular structures, passing near the ROI. The needle of such geometry does not demand the reduction of laser power in order to prevent injury to the nearby vital tissues and organs. The orientation of this needle in a tissue strongly determines the heated area. Moreover, such configuration could be optimized for the formation of a bent light beam, such as the Airy beam or the

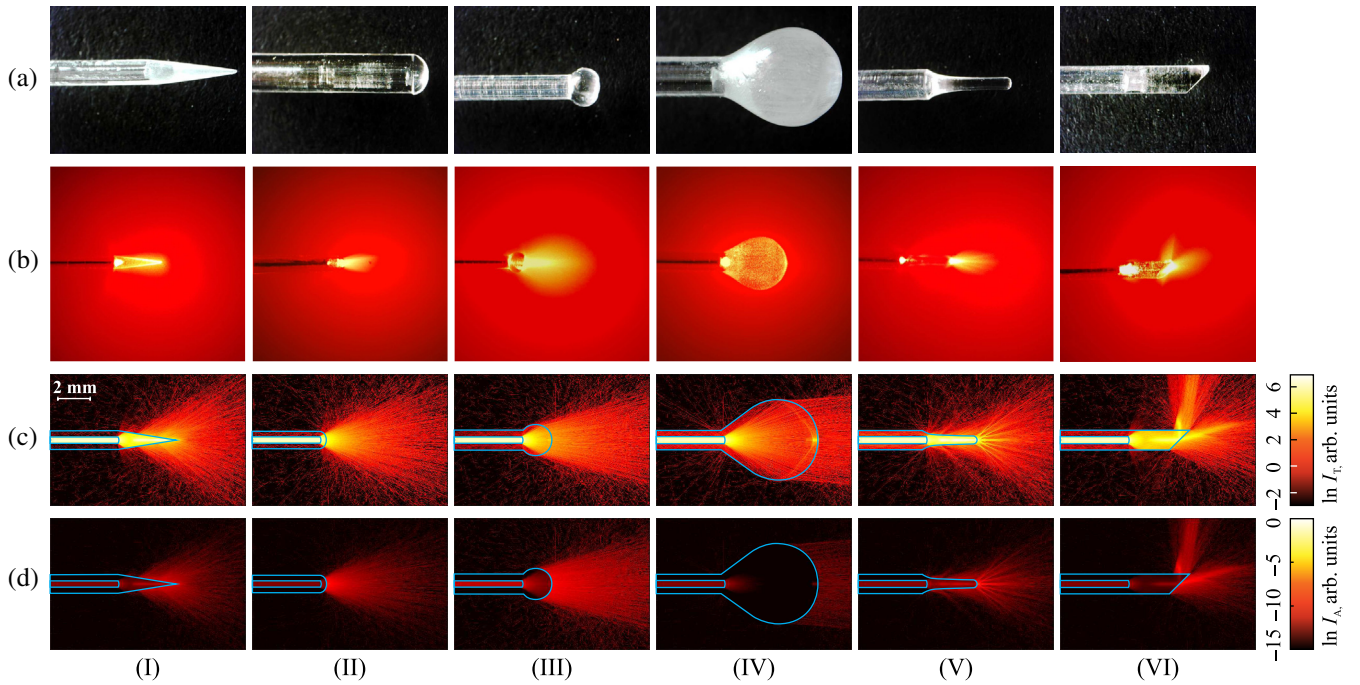

Fig. 4 Examples and application of sapphire capillary needles for light delivery. (a) Pictures of the fabricated sapphire tips; (b) pictures of laser light ($\lambda = 632.8$ nm) distribution produced by the sapphire tips in a diluted intralipid solution; the results of the numerical simulation of laser light distribution in a tissue phantom, corresponding to the (c) transmitted ln I_T and (d) absorbed ln I_A intensities. The dimensions of needles used in simulations match the dimensions of the fabricated ones.

photonic hook[53,54] (i.e., the near-field curved light beam with the waist smaller than the wavelength). We summarize the main listed properties of the considered sapphire needles in Table 1.

Due to the high thermal and chemical resistance and high hardness, the as-grown or mechanically treated form of a sapphire needle is very stable; thus, the radiation pattern produced by a specific tip tends to be reproducible in time and minimizes the uncontrolled effects, such as carbonization. It opens a wide perspective for shaping the needle tips, particularly, making various cone angles, and applying them for interstitial treatment with no fear of impact of the surface and shape defects.

Table 1 A summary of the properties featured by the considered sapphire needle tips.

Needle type	I	II	III	IV	V	VI
Radiation pattern properties						
Anisotropy	Low	High	High	High	High	High
Diffused light	✓	—	—	—	✓	—
Collimated light	—	—	—	✓	—	—
Axial symmetry	✓	✓	✓	✓	✓	—
Aside irradiation	—	—	—	—	—	✓
Applications						
Interstitially	✓	✓	—	—	✓	✓
Percutaneously	✓	✓	✓	✓	✓	—

In order to observe the range of possible light distributions formed by a pointed sapphire needle, we apply numerical simulations for six variations of the needle cone, i.e., the length of the pointed part has the values $l = 0.6$, 2.0, 4.0, 6.0, 8.0, and 10.0 mm (the corresponding cone angle $\theta \approx 90$ deg, 33.4 deg, 17 deg, 11.4 deg, 8.6 deg, and 6.9 deg). The considered needles have 500-μm-diameter capillary channels; the optical parameters are listed above in this paragraph. The results are presented in Fig. 5. One can observe that the large angle leads to forward-propagated laser light; moreover, such pointed needle could provide some kind of a Bessel beam of a first order with its benefits of low-diffraction caustic;[55–57] in turn the small angle might lead to the extreme light confinement and, thus, to a specific localization of tissue exposure. It is interesting that the needle with $l = 2.0$ mm combines diffused and forward components simultaneously. Thus changing the cone angle, one can select a needle for a specific ROI and purpose.

4 Discussion

Although in this work we considered a limited set of the sapphire capillary needles, there are many more options for their design. Particularly, the considered sapphire needles can be combined either with the conventional flat cleaved or diffusing optical fibers.[14,28,31,36,38–40,58,59] The surface of diffusing fiber is partly matt at the end enabling both forward and lateral irradiation and ensuring a uniform irradiation of a large tissue volume. Additionally, a fiber can be moved along the channel inside a rigidly fixed needle during the tissue exposure. It is also possible to form a diffusive sapphire surface in a capillary channel. The latter configuration should lead to more uniform light distribution in tissue, if necessary, and to minimization of the overheating risk.

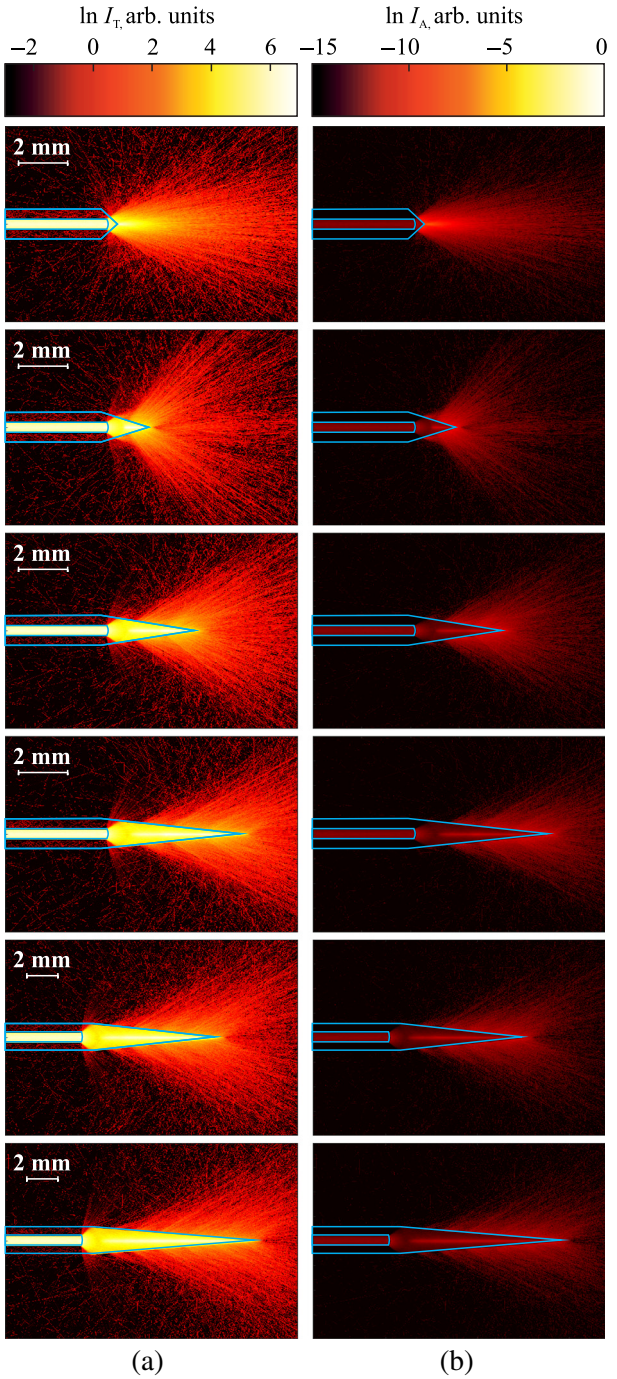

Fig. 5 Numerical simulation of light ($\lambda = 632.8$ nm) distribution in a tissue phantom with $n_p = 1.33$, $\mu_a = 10^{-4}$ mm^{-1}, $\mu_s = 0.2$ mm^{-1}, formed by the pointed sapphire capillary needles with diameter 1.2 mm; (a) transmitted intensity ln I_T (b) absorbed intensity ln I_A. The lengths of cone part correspond to 0.6, 2.0, 4.0, 6.0, 8.0, and 10.0 mm (from top to bottom).

We should note that an intraoperative monitoring of the correct input and interstitial position of the needle during a therapeutic procedure remains challenging. Indeed, the conditions of tissues exposure to laser radiation depend on the considered tissue type, may vary from patient to patient, and usually feature a dynamic character due to the light-induced changes in tissues. In order to resolve this problem, nowadays, the modern modalities of tissue imaging, such as intraoperative ultrasound imaging, magnetic resonance imaging (MRI), and MR-based thermometry are increasingly applied in a clinical practice.[16,23,25,29,34,58,60–64] Since the considered sapphire capillary needles provide an ability to deliver electromagnetic radiation, with a broad range of wavelengths, to hardly accessible tissues and internal organs, it is possible to use electromagnetic waves from different spectral ranges for the interstitial exposure and diagnosis using the sapphire needles, opening new ways of multimodal applications. For example, we could easily combine, in a single instrument, tissue exposure to laser radiation, fluorescence diagnostics of tissues, and ultrasound monitoring of the needle position during the medical procedure. Another option is to use sapphire needles in MRI-guided interstitial therapy and diagnosis, since sapphire is a nonmagnetic material.

A prediction of the exposed and ablated regions of tissues remains a complicated problem of the interstitial therapy, mainly due to a complex structure of tissues and to a strong variation of their properties. Nevertheless, modeling of heating process during LITT and I-PDT, for example, by means of radiation transfer theory and the statistical Monte-Carlo methods, demonstrates quite satisfactory results.[26,63] Such preliminary modeling can help one to choose the appropriate needle tip geometry, which might be produced by the EFG and the related technologies of sapphire shaped crystal growth. It opens a wide range of opportunities for planning the treatment, including the treatment of a region with irregular form.

In contrast to glass protecting caps and bare fibers, the complex sapphire tips maintain their shape and surface quality unaltered during the exposure and would not lead to undesirable effects and errors. The melting temperature of sapphire is 2053°C, whereas the maximum operating temperature is 1800°C, which is far beyond the applied temperatures during LTT and PDT.[48] This enables high stability of the needle shape during laser exposure, even when the tip has rather complex form. Thanks to strong chemical inertness and heat resistance of sapphire medical instruments, they allow for multiple sterilizations without a decline of their performance. Actually, the cost of EFG-grown sapphire capillary needle is comparable with the cost of diffusing silica fiber. Therefore, such needles can be disposable as well as reusable. Moreover, since the applied fiber is protected from the direct contact with tissue, it also can be used multiple times. All the aforementioned could lead to significant reduction of the treatment expenses.

We have demonstrated several examples of sapphire needles and described their abilities in LITT and I-PDT; however, the further full-blown *ex vivo* and *in vivo* studies are required in order to completely characterize these promising types of medical instruments and to reveal their benefits and weaknesses.

5 Conclusion

In this work, we have studied the potential of the sapphire capillary needles grown by the EFG technique to form different radiation patterns by changing their tip geometry. They could replace the currently used silica introducers and bare fibers for PDT and LTT, since sapphire needles demonstrate high thermal and chemical stability, are reusable and admit multiple sterilization, protect optical fiber from the direct contact with tissue, additionally, their cost is comparable with the disposable diffusing silica fiber. We demonstrated a set of fabricated examples of such needles with internal capillary channels, closed at the one side, for placing the optical fiber inside. The EFG technique enables making different tips of the needles with minimal or even without mechanical treatment. Both the as-grown and

mechanically treated tips were studied experimentally, using He–Ne laser and tissue phantoms, and numerically, using Monte-Carlo modeling. We observed a good agreement between the numerical and experimental results. It opens a wide perspective for adjusting the medical instrument for particular patient and conditions, applying preliminary numerical modeling. We have shown a variety of possible radiation patterns that can be applied according to the stated treatment purpose. The demonstrated set of radiation patterns ranged from forward collimated to diffused and aside propagated light, and together cover the treatment of tissues of rather different volumes and shapes.

Nevertheless, the further investigations of such instruments should be done. It is essential to estimate *ex vivo* and *in vivo* the impact of small variations of the tip form on the volume of treated tissue and rigorously specify the operational regimes, including maximal and minimal applied laser powers and expositions for different tissue types. The advantages of the EFG-grown sapphire capillary needles, particularly, the potential for interstitial diagnosis and combined diagnosis with laser treatment open the novel perspectives in the further improvement of laser therapeutic methods in clinics.

Disclosures

The authors have no relevant financial interests in this article and no potential conflicts of interest to disclose.

Acknowledgments

The development, fabrication, and experimental study of sapphire needles were supported by the grant from the Russian Foundation for Basic Research (RFBR), Project No. 18-38-20140. The preparation and application of tissue phantoms were supported by the RFBR, Project No. 18-08-01230.

References

1. M. Niemz, *Laser-Tissue Interactions. Fundamentals and Applications*, Springer-Verlag Berlin Heidelberg, New York (2002).
2. S. G. Bown, "Phototherapy of tumors," *World J. Surg.* **7**(6), 700–709 (1983).
3. M. R. Hamblin and Y. Huang, *Handbook of Photomedicine*, 1st ed., CRC Press, Boca Raton, Florida (2013).
4. S. Thomsen, "Pathologic analysis of photothermal and photomechanical effects of laser–tissue interactions," *Photochem. Photobiol.* **53**(6), 825–835 (1991).
5. A. J. Welch and M. J. van Gemert, *Optical-Thermal Response of Laser-Irradiated Tissue*, 2nd ed., Springer Science + Business Media, Berlin, Germany (2011).
6. B. C. Wilson and M. S. Patterson, "The physics, biophysics and technology of photodynamic therapy," *Phys. Med. Biol.* **53**(9), R61–R109 (2008).
7. K. Svanberg et al., "Photodynamic therapy: superficial and interstitial illumination," *J. Biomed. Opt.* **15**(4), 041502 (2010).
8. R. Cavaliere et al., "Selective heat sensitivity of cancer cells. Biochemical and clinical studies," *Cancer* **20**(9), 1351–1381 (1967).
9. N. Ikeda et al., "New aspects of photodynamic therapy for central type early stage lung cancer," *Lasers Surg. Med.* **43**(7), 749–754 (2011).
10. Z. Huang et al., "Photodynamic therapy for treatment of solid tumors—potential and technical challenges," *Technol. Cancer Res. Treat.* **7**(4), 309–320 (2008).
11. R. Darlenski and J. W. Fluhr, "Photodynamic therapy in dermatology: past, present, and future," *J. Biomed. Opt.* **18**(6), 061208 (2012).
12. O. Semyachkina-Glushkovskaya et al., "Photodynamic opening of blood-brain barrier," *Biomed. Opt. Express* **8**(11), 5040–5048 (2017).
13. E. Borisova et al., "Photodiagnosis and photodynamic therapy of cutaneous melanoma," Chapter 7 in *Current Management of Malignant Melanoma*, M. Y. Cao, Ed., pp. 141–156, IntechOpen, London (2011).
14. V. G. Truong et al., "Effect of spatial light distribution on the thermal response of vascular tissue," *Biomed. Opt. Express* **9**(7), 3037–3048 (2018).
15. J. Hwang et al., "Ex vivo laser lipolysis assisted with radially diffusing optical applicator," *J. Biomed. Opt.* **21**(5), 058001 (2016).
16. J. Y. Kang et al., "Laser interstitial thermal therapy for medically intractable mesial temporal lobe epilepsy," *Epilepsia* **57**(2), 325–334 (2016).
17. P. Saccomandi et al., "Temperature monitoring and lesion volume estimation during double-applicator laser-induced thermotherapy in ex vivo swine pancreas: a preliminary study," *Lasers Med. Sci.* **29**(2), 607–614 (2014).
18. H. Yu and C. T. Burke, "Comparison of percutaneous ablation technologies in the treatment of malignant liver tumors," *Semin. Interventional Radiol.* **31**, 129–137 (2014).
19. W. van den Bos et al., "Focal therapy in prostate cancer: international multidisciplinary consensus on trial design," *Eur. Urol.* **65**(6), 1078–1083 (2014).
20. J. P. Ritz et al., "Laser-induced thermotherapy for lung tissue—evaluation of two different internally cooled application systems for clinical use," *Lasers Med. Sci.* **23**(2), 195–202 (2008).
21. K. Haraldsdóttir et al., "Interstitial laser thermotherapy (ILT) of breast cancer," *Eur. J. Surg. Oncol.* **34**(7), 739–745 (2008).
22. R. L. Hood et al., "Intracranial hyperthermia through local photothermal heating with a fiberoptic microneedle device," *Lasers Surg. Med.* **45**(3), 167–174 (2013).
23. J. H. Sherman et al., "Neurosurgery for brain tumors: update on recent technical advances," *Curr. Neurol. Neurosci. Rep.* **11**(3), 313–319 (2011).
24. A. H. Hawasli et al., "Stereotactic laser ablation of high-grade gliomas," *Neurosurg. Focus* **37**(6), E1 (2014).
25. G. Shafirstein et al., "Irradiance controls photodynamic efficacy and tissue heating in experimental tumours: implication for interstitial PDT of locally advanced cancer," *Br. J. Cancer* **119**(10), 1191–1199 (2018).
26. E. Oakley et al., "Surface markers for guiding cylindrical diffuser fiber insertion in interstitial photodynamic therapy of head and neck cancer," *Lasers Surg. Med.* **49**(6), 599–608 (2017).
27. G. Shafirstein et al., "Interstitial photodynamic therapy—a focused review," *Cancers* **9**(2), 12 (2017).
28. C. Germer et al., "Diffusing fibre tip for the minimally invasive treatment of liver tumours by interstitial laser coagulation (ILC): an experimental ex vivo study," *Lasers Med. Sci.* **14**(1), 32–39 (1999).
29. T. Bretschneider et al., "Image-guided high-dose-rate brachytherapy of malignancies in various inner organs—technique, indications, and perspectives," *J. Contemp. Brachyther.* **8**(3), 253–263 (2016).
30. M. Sharma et al., "Laser interstitial thermal therapy in the management of brain metastasis and radiation necrosis after radiosurgery: an overview," *Expert Rev. Neurother.* **16**(2), 223–232 (2016).
31. G. Keiser et al., "Review of diverse optical fibers used in biomedical research and clinical practice," *J. Biomed. Opt.* **19**(8), 080902 (2014).
32. N. T. Pham et al., "Real-time temperature monitoring with fiber Bragg grating sensor during diffuser-assisted laser-induced interstitial thermotherapy," *J. Biomed. Opt.* **22**(4), 045008 (2017).
33. A. Fasano, D. Hömberg, and D. Naumov, "On a mathematical model for laser-induced thermotherapy," *Appl. Math. Modell.* **34**(12), 3831–3840 (2010).
34. B. Bazrafshan et al., "Temperature imaging of laser-induced thermotherapy (LITT) by MRI: evaluation of different sequences in phantom," *Lasers Med. Sci.* **29**(1), 173–183 (2014).
35. C. Pantaleone, S. Dymling, and J. Axelsson, "Optical fiber solutions for laser ablation of tissue and immunostimulating interstitial laser thermotherapy—product development in the network of developers, industry and users," *Photonics Lasers Med.* **5**(1), 69–75 (2015).
36. T. Vo-Dinh, *Biomedical Photonics Handbook: Therapeutics and Advanced Biophotonics*, CRC Press, Boca Raton (2015).
37. T. Eguro et al., "Energy output reduction and surface alteration of quartz and sapphire tips following Er:YAG laser contact irradiation for tooth enamel ablation," *Lasers Surg. Med.* **41**(8), 595–604 (2009).
38. M. D. Stringasci et al., "Interstitial PDT using diffuser fiber—investigation in phantom and in vivo models," *Lasers Med. Sci.* **32**(5), 1009–1016 (2017).
39. R. M. Verdaasdonk and C. F. P. van Swol, "Laser light delivery systems for medical applications," *Phys. Med. Biol.* **42**(5), 869–894 (1997).

40. P. H. Möller et al., "Interstitial laser thermotherapy: comparison between bare fibre and sapphire probe," *Lasers Med. Sci.* **10**(3), 193–200 (1995).
41. V. N. Kurlov et al., "Shaped crystal growth," Chapter 5 in *Crystal Growth Processes Based on Capillarity: Czochralski, Floating Zone, Shaping and Crucible Techniques*, T. Duffar, Ed., pp. 277–354, John Wiley & Sons, Chippenham, Wiltshire (2010).
42. H. E. LaBelle and A. I. Mlavsky, "Growth of controlled profile crystals from the melt: part I—sapphire filaments," *Mater. Res. Bull.* **6**(7), 571–579 (1971).
43. H. E. LaBelle, "Growth of controlled profile crystals from the melt: part II—edge-defined, film-fed growth (EFG)," *Mater. Res. Bull.* **6**(7), 581–589 (1971).
44. B. Chalmers, H. E. LaBelle, and A. I. Mlavsky, "Growth of controlled profile crystals from the melt: part III—theory," *Mater. Res. Bull.* **6**(8), 681–690 (1971).
45. I. A. Shikunova et al., "Sapphire needle capillaries for laser medicine," *Bull. Russ. Acad. Sci.* **73**(10), 1345–1348 (2009).
46. P. I. Antonov and V. N. Kurlov, "A review of developments in shaped crystal growth of sapphire by the Stepanov and related techniques," *Prog. Cryst. Growth Charact. Mater.* **44**(2), 63–122 (2002).
47. N. V. Abrosimov, V. N. Kurlov, and S. N. Rossolenko, "Automated control of Czochralski and shaped crystal growth processes using weighing techniques," *Prog. Cryst. Growth Charact. Mater.* **46**(1–2), 1–57 (2003).
48. G. Katyba et al., "Sapphire shaped crystals for waveguiding, sensing and exposure applications," *Prog. Cryst. Growth Charact. Mater.* **64**(4), 133–151 (2018).
49. V. V. Tuchin, *Tissue Optics: Light Scattering Methods and Instruments for Medical Diagnostics*, 3rd ed., SPIE Press, Bellingham, Washington (2015).
50. H. J. van Staveren et al., "Light scattering in Intralipid-10% in the wavelength range of 400–1100 nm," *Appl. Opt.* **30**(31), 4507–4514 (1991).
51. F. Pisanello et al., "Dynamic illumination of spatially restricted or large brain volumes via a single tapered optical fiber," *Nat. Neurosci.* **20**, 1180–1188 (2017).
52. J. M. Stujenske, T. Spellman, and J. A. Gordon, "Modeling the spatiotemporal dynamics of light and heat propagation for in vivo optogenetics," *Cell Rep.* **12**(3), 525–534 (2015).
53. I. V. Minin et al., "Experimental observation of a photonic hook," *Appl. Phys. Lett.* **114**(3), 031105 (2019).
54. L. Yue et al., "Photonic hook: a new curved light beam," *Opt. Lett.* **43**(4), 771–774 (2018).
55. G. Sokolovskii et al., "Bessel beams from semiconductor light sources," *Prog. Quantum Electron.* **38**(4), 157–188 (2014).
56. T. Vettenburg et al., "Light-sheet microscopy using an Airy beam," *Nat. Methods* **11**, 541–544 (2014).
57. D. Tarrazo-Serrano et al., "Design of acoustical Bessel-like beam formation by a pupil masked Soret zone plate lens," *Sensors* **19**(2), 378 (2019).
58. H. Atsumi et al., "Novel laser system and laser irradiation method reduced the risk of carbonization during laser interstitial thermotherapy: assessed by MR temperature measurement," *Lasers Surg. Med.* **29**(2), 108–117 (2001).
59. V. G. Truong et al., "Spatial effect of conical angle on optical-thermal distribution for circumferential photocoagulation," *Biomed. Opt. Express* **8**(12), 5663–5674 (2017).
60. K. V. Larin, I. V. Larina, and R. O. Esenaliev, "Monitoring of tissue coagulation during thermotherapy using optoacoustic technique," *J. Phys. D Appl. Phys.* **38**(15), 2645–2653 (2005).
61. R. Rammo et al., "MR-guided laser interstitial thermal therapy in the treatment of recurrent intracranial meningiomas," *Lasers Surg. Med.* **51**(3), 245–250 (2019).
62. I. Karampelas and A. E. Sloan, "Laser-induced interstitial thermotherapy of gliomas," *Prog. Neurol. Surg.* **32**, 14–26 (2018).
63. F. Hübner et al., "Validation of a mathematical model for laser-induced thermotherapy in liver tissue," *Lasers Med. Sci.* **32**(6), 1399–1409 (2017).
64. M. Zhu, Z. Sun, and C. K. Ng, "Image-guided thermal ablation with MR-based thermometry," *Quant. Imaging Med. Surg.* **7**(3), 356–368 (2017).

Biographies of the authors are not available.